Supplementary file

Correspondence to: Marion Roger (marion.roger@univ-grenoble-alpes.fr)

1 AFT supplementary figure:

From supplementary figure S1, we discriminate the reset and partially reset samples from the non-reset samples (S1, a). CAR19-061 is the only non-reset samples we have in our set, but CAR19-045 and CAR19-066 are very close to the limit and the 2σ error fall in the left part of the limit line. Repartition of the AFT age as a function of the elevation of the sampling site mark a pattern of increased altitude for older ages, apart from the samples from Magura nappe (i.e., CAR19-061 and CAR19-066). The difference in elevation is low (≈ 500m) for our data set. Usually more elevated samples tend to have younger ages due to the thermal regime in mountains belt where elevated area possess higher heat production (concentration of crust material in the high elevated areas) and faster heat advection (by active topography building and thrusting/fault activity). Strikingly the oldest and highest samples are beared in the more external nappes (Krosno and Skyba nappes) and as elevation decrease, the youngest samples are toward the internal nappes (Burkut and Dukla nappes). The Magura nappe, which is the back stop of our wedge, is showing the oldest ages and the lowest elevation in the dataset, implying less burial coupled with a longer period of exposition to erosion for this nappe. For the rest of the units, the increase of age toward the outer belt and the higher elevation is coherent with the dynamic of the retreating subduction zone and a thermally “immature” wedge building in the Ukrainian Carpathians (Dahlen et al., 1984; Royden, 1993a, b; Willett and Brandon, 2002; Husson and Moretti, 2002). The mean track length (MTL) compared to the age of the AFT samples don’t display any pattern of shorter tracks in younger samples. High dispersion (> 30%) is present for all our samples (except for CAR19-068 with 25% and CAR19-062 with 29%) and samples often show two to three grain populations. This high difference inside each sample can lead to no correlation in track length measurement and AFT age, especially when track length measurement is low (in our case no more than 21 track measured in a sample).

2 AHe and ZHe supplementary figure:

AHe single-grain age from our study show non-reset ages (CAR19-066_a2 and for CAR19-072_a2) and some partial reset ages (see A1 a), c) and e)). Most of the AHe ages are around 10 Ma when reset. The AHe with ages close to the CA of the corresponding AFT can be the result of the differential annealing between the grain population (this is the case for sample CAR19-061, -066 and -072). Comparing the ESR (equivalent spherical radius) and the eU (equivalent Uranium content) to the AHe single-grain age show no correlation of these parameters. Old AHe ages are in the mean range for the eU content (10-60 ppm) and the ESR (60-80 µm) and AHe ages around 10 Ma pertain the maximum and minimum in both characteristics. Sample CAR19-068 has the smallest differences among grains for eU and ESR, in accordance with a single population in AFT ages (25 % of dispersion).

ZHe ages compared to the stratigraphic age (A1 b)) show the clear non-reset of the thermochronometer in our data. We also identified a population of ages around 100 Ma, and one older ranging from 200 – 400 Ma. As for AHe single grain, there are no evident correlations between the ZHe ages and ESR or eU content. It is worth noticing that for zircons, CAR19-068 show a larger dispersion of grains characteristics, unlike CAR19-061 and CAR19-062 that display great similarities between grains (except for CAR19-061_z4) which do not show for the apatite grains.

References

Dahlen, F. A., Suppe, J., and Davis, D.: Mechanics of fold-and-thrust belts and accretionary wedges: Cohesive Coulomb Theory, J. Geophys. Res., 89, 10087–10101, https://doi.org/10.1029/JB089iB12p10087, 1984.

Husson, L. and Moretti, I.: Thermal regime of fold and thrust belts—an application to the Bolivian sub Andean zone, Tectonophysics, 345, 253–280, https://doi.org/10.1016/S0040-1951(01)00216-5, 2002.

Royden, L. H.: The steady state thermal structure of eroding orogenic belts and accretionary prisms, J. Geophys. Res., 98, 4487–4507, https://doi.org/10.1029/92JB01954, 1993a.

Royden, L. H.: The tectonic expression slab pull at continental convergent boundaries, Tectonics, 12, 303–325, https://doi.org/10.1029/92TC02248, 1993b.

Willett, S. D. and Brandon, M. T.: On steady states in mountain belts, Geol, 30, 175, https://doi.org/10.1130/0091-7613(2002)030<0175:OSSIMB>2.0.CO;2, 2002.

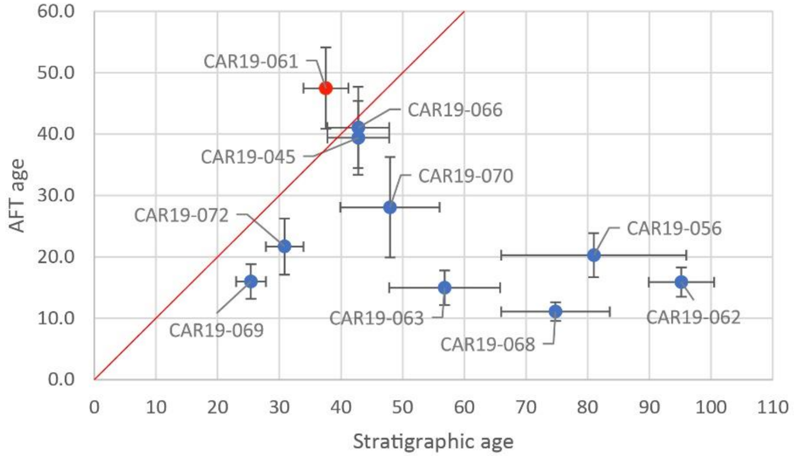

CAR19-061
CAR19-066
CAR19-045
CAR19-070
CAR19-072
CAR19-056
CAR19-062
CAR19-063
CAR19-068
CAR19-069
AFT age
Stratigraphic age

a

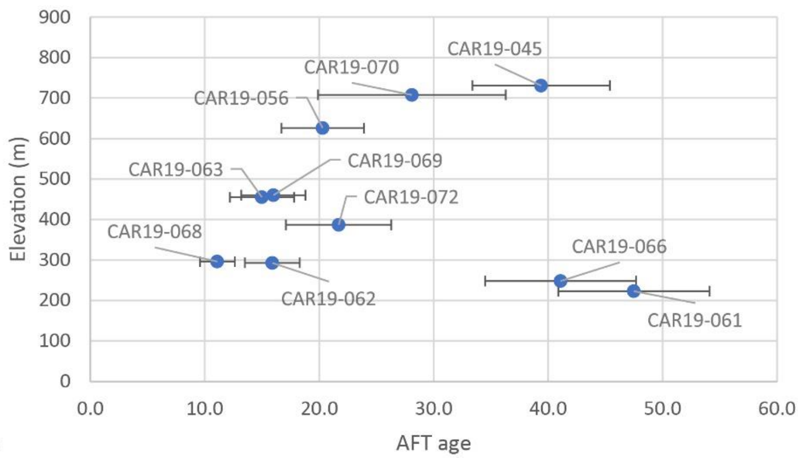

CAR19-045
CAR19-070
CAR19-056
CAR19-063
CAR19-069
CAR19-072
CAR19-068
CAR19-066
CAR19-062
CAR19-061
Elevation (m)
AFT age

b

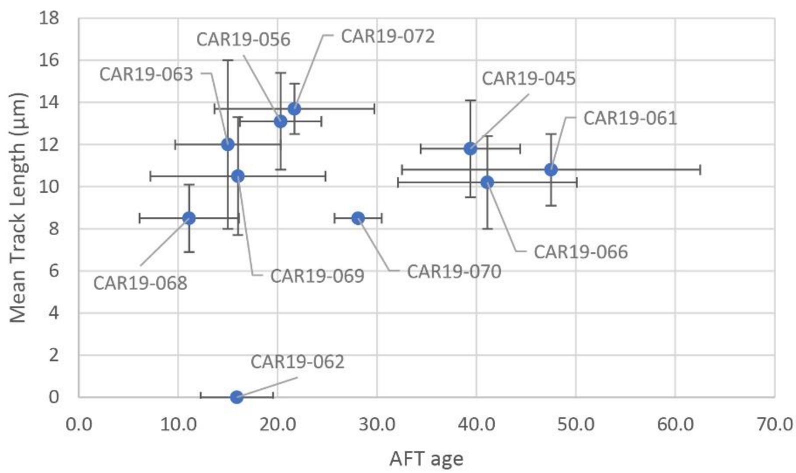

CAR19-056
CAR19-072
CAR19-063
CAR19-045
CAR19-061
CAR19-066
CAR19-068
CAR19-069
CAR19-070
CAR19-062
Mean Track Length (µm)
AFT age

c

S 1: a) Graphic of AFT age vs. Stratigraphic age, both scales are in My. The red line shows the delimitation for: on the left non-reset samples (here only CAR19-061); on the right reset and partially reset samples. CAR19-045 and CAR19-066 samples display very poor partial resetting compared to the reset of the "reset" samples. b) AFT age vs. Elevation of the sampling site. Elevation and topography are supposed to have remained low in the Ukrainian Carpathians region. The older AFT ages are at a higher elevation in our case, is we speak in terms of nappes, the external nappes Krosno and Skyba (CAR19-045, -056, -069, -070, -072) have higher elevation and older AFT central age. Burkut and Dukla samples (CAR19-062, -063, -068) are more internal and les elevated but also younger for AFT thermochronometer. The samples out of the trend of younger AFT ages toward low elevation are the samples from Magura nappe (CAR19-061, -066), both showing non-rest or very poor partial resetting. c) AFT age vs. Mean track length (CAR19-062 has no track length counted). Mean track length should align with the degree of resetting of each sample i.e., annealing of tracks is due to higher burial temperature or long residence at the PAZ, and should correspond to higher degree of resetting of the AFT. This pattern isn't obvious in our dataset. Non-reset, or very poorly reset sample (CAR19-061, -066, -045) have MTL of 10-12 µm, comparable to the MTL of CAR19-063 and CAR19-069, which display more resetting.

Sample	mineral	Ft corrected Age, Ma	2s analytic err., Ma	weighted 2s analytic err., Ma	U (ppm)	Th (ppm)	147Sm (ppm)	[U]e	Th/ 238U	He (nmol/g)	mass (ug)	Ft	ESR (mm)
Dur930_a1	Apatite	40.6410	1.5143	1.0937	1.6224	27.5233	3.6929	8.0903	17.5284	1.7959	37.5024	1.0000	121.8247
Dur930_a2	Apatite	30.6691	1.1054	0.8652	3.5240	70.2528	8.9501	20.0334	20.5975	3.3550	25.3718	1.0000	107.0631
Dur930_a3	Apatite	29.6255	0.3847	0.2803	3.6537	64.1073	7.3323	18.7189	18.1287	3.0262	33.7372	1.0000	115.2892
CAR19-63_a1	Apatite	9.3098	0.4653	0.2995	5.9116	18.7023	3.8020	10.3066	3.2687	0.4069	6.5145	0.7808	68.4279
CAR19-62_a1	Apatite	41.0700	1.0824	0.6261	11.9649	44.8312	22.0715	22.5002	3.8713	4.0394	8.3652	0.7990	74.6325
CAR19-62_a2	Apatite	10.7433	0.5395	0.3764	10.9541	88.9777	4.0780	31.8638	8.3926	1.4163	5.1058	0.7615	62.8878
CAR19-62_a3	Apatite	3.4658	0.2089	0.1355	1.7702	45.4976	5.3992	12.4622	26.5551	0.1859	7.1869	0.7890	71.0808
CAR19-56_a1	Apatite	9.7806	0.3043	0.1691	24.6810	78.8466	48.6459	43.2099	3.3007	1.7365	4.6311	0.7519	60.4649
CAR19-56_a2	Apatite	9.1818	0.3653	0.2125	44.7140	180.2646	22.6570	87.0762	4.1654	3.3541	5.9541	0.7727	65.9914
CAR19-56_a3	Apatite	8.9343	0.2880	0.1100	136.8446	194.3596	60.2509	182.5191	1.4675	6.6015	4.3863	0.7471	59.3007
CAR19-69_a1	Apatite	12.1729	0.3960	0.1241	34.8693	116.1868	7.4685	62.1732	3.4427	3.2048	6.4073	0.7811	68.5161
CAR19-69_a2	Apatite	9.6729	0.2208	0.1316	19.7150	79.9881	8.7512	38.5122	4.1919	1.6454	10.4309	0.8137	80.5269
CAR19-69_a3	Apatite	13.8216	0.2591	0.1614	37.6026	82.7747	44.5435	57.0546	2.2744	3.4600	9.4982	0.8056	77.1795
CAR19-45_a1	Apatite	8.1836	0.2041	0.1793	7.6135	18.5761	16.5109	11.9789	2.5209	0.4199	6.7071	0.7829	69.0783
CAR19-45_a2	Apatite	17.0282	0.9147	0.5099	4.4731	36.0914	13.1468	12.9546	8.3365	0.9134	4.9951	0.7564	61.5710
CAR19-45_a3	Apatite	9.1607	0.3834	0.2432	10.4214	68.1773	24.7579	26.4430	6.7593	1.0989	15.3844	0.8300	88.2276
CAR19-47_a1	Apatite	0.1376	0.1018	0.1006	9.3638	2.1437	60.8062	9.8675	0.2365	0.0062	9.0567	0.8049	76.8677
CAR19-47_a2	Apatite	9.5252	0.1954	0.1369	25.3028	31.6357	17.6197	32.7372	1.2918	1.4045	13.7679	0.8299	88.1766
CAR19-47_a3	Apatite												58.9836
CAR19-72_a1	Apatite	18.3523	0.7660	0.6159	7.5814	22.9412	11.7066	12.9726	3.1265	1.0064	5.9513	0.7746	66.5509
CAR19-72_a2	Apatite	29.5703	1.2009	0.3223	35.0301	5.1192	21.7665	36.2331	0.1510	4.6153	7.9205	0.7934	72.6115
0	Apatite												
CAR19-68_a1	Apatite	6.5524	0.2327	0.1858	15.9909	387.7030	52.7088	107.1011	25.0504	2.9204	5.4076	0.7623	63.1033
CAR19-68_a2	Apatite	7.1685	0.3440	0.2577	22.4447	291.8276	39.0549	91.0242	13.4338	2.7653	6.3322	0.7774	67.3988
CAR19-68_a3	Apatite	7.0698	0.1375	0.1116	27.5763	345.8539	44.8668	108.8519	12.9582	3.1739	4.8811	0.7568	61.6704
CAR19-61_a1	Apatite	14.5630	0.9784	0.7508	4.4300	28.1176	41.0434	11.0376	6.5579	0.6532	3.4885	0.7268	54.9090
CAR19-61_a2	Apatite	14.7863	0.7559	0.5105	6.5782	13.6280	23.1122	9.7808	2.1405	0.6074	5.1637	0.7615	62.8820
CAR19-61_a3	Apatite	26.9930	1.0998	0.6561	14.6078	5.4670	9.1366	15.8926	0.3867	1.7545	4.5442	0.7533	60.8114
CAR19-66_a1	Apatite	12.9991	0.4361	0.2163	44.9248	128.3676	6.8123	75.0912	2.9523	4.1610	7.3172	0.7867	70.3385
CAR19-66_a2	Apatite	54.9751	1.6715	0.7189	29.1782	22.0699	21.6131	34.3646	0.7815	8.0182	6.7318	0.7791	67.9059
CAR19-66_a3	Apatite	9.0592	0.6903	0.4977	7.4556	41.6717	12.3364	17.2484	5.7749	0.6155	3.3438	0.7223	54.0127

S2: Table of raw result for AHe

Sample	mineral	Ft corrected Age, Ma	2s analytic err., Ma	weighted 2s analytic err., Ma	U (ppm)	Th (ppm)	147Sm (ppm)	[U]e	Th/ 238U	He (nmol/g)	mass (ug)	Ft	ESR (mm)
FCT102020_z1	zircon	33.0779	7.5619	0.5257	321.8962	234.3351	0.6548	376.9649	0.7522	45.8849	3.0250	0.6803	37.7482
FCT102020_z2	zircon	31.3226	1.9049	0.3733	170.1877	108.8041	0.3445	195.7567	0.6605	26.7201	8.2809	0.8058	64.3600
CAR19-45_z1	zircon	23.2087	2.6997	0.5494	1.8720	23.7099	0.5864	7.4438	13.0863	0.7789	9.4819	0.8290	79.4660
CAR19-45_z2	zircon	11.0089	4.7565	2.4292	0.7659	5.3431	0.3388	2.0215	7.2083	0.0933	5.8554	0.7714	57.6151
CAR19-45_z3	zircon	298.5007	14.4691	2.3075	483.7465	74.9364	0.6139	501.3565	0.1601	704.9022	17.0114	0.8506	83.6214
CAR19-47_z1	zircon	417.4372	11.6336	2.6335	66.0032	62.7623	0.4220	80.7523	0.9825	164.9278	25.4927	0.8763	105.4407
CAR19-47_z2	zircon	229.0865	35.9548	4.7439	54.1031	73.8241	0.6663	71.4518	1.4098	71.4482	6.6352	0.7941	61.4000
CAR19-56_z1	zircon	491.6974	131.7172	15.6788	52.3130	77.3411	0.5332	70.4882	1.5275	150.1569	4.8454	0.7726	55.3641
CAR19-56_z2	zircon	14.5933	1.0015	0.7795	2.3507	70.0850	2.5334	18.8207	30.8048	1.2061	8.6971	0.8063	70.7670
CAR19-56_z3	zircon	432.2861	8.9814	4.8452	98.7732	123.3666	1.0325	127.7643	1.2905	259.7290	14.9714	0.8419	80.8705
CAR19-56_z4	zircon	328.7016	13.6658	3.3071	41.7588	25.1998	0.1921	47.6807	0.6235	71.8003	10.7437	0.8259	72.1294
CAR19-61_z1	zircon	113.2196	7.9114	0.8262	212.4424	61.1805	0.3456	226.8198	0.2975	111.2387	6.6005	0.7956	60.4300
CAR19-61_z2	zircon	89.5871	2.9808	0.9347	274.9460	132.0132	0.6069	305.9691	0.4961	121.2298	9.7467	0.8139	67.0477
CAR19-61_z3	zircon	85.3967	6.8046	0.7392	269.5291	58.3756	0.4471	283.2473	0.2238	106.0204	9.0958	0.8071	64.1158
CAR19-61_z4	zircon	91.6023	10.4021	0.4673	853.1514	260.7592	1.2641	914.4299	0.3158	364.1913	6.5445	0.8001	61.9002
CAR19-61_z5	zircon	117.6210	21.2997	1.2492	111.4603	43.7683	0.5569	121.7459	0.4057	63.2141	8.3012	0.8104	65.6077
CAR19-62_z1	zircon	128.5603	82.7970	1.3623	47.0322	35.7300	0.3093	55.4287	0.7849	31.5564	8.8623	0.8121	66.8114
CAR19-62_z2	zircon	112.4478	7.9154	1.7741	204.8089	190.1343	2.4967	249.4904	0.9592	120.6091	5.2782	0.7893	61.8883
CAR19-62_z3	zircon	128.6948	13.6738	1.3362	74.5673	111.7824	0.3609	100.8362	1.5489	58.2647	9.4946	0.8232	72.2393
0	zircon												
CAR19-62_z5	zircon	114.0263	10.5994	1.5466	167.8298	55.6044	0.5294	180.8968	0.3423	87.8688	6.3486	0.7823	56.6021
CAR19-63_z1	zircon	89.0035	8.2054	0.7706	39.9423	51.3777	0.1557	52.0160	1.3290	20.8521	10.4026	0.8284	76.5229
CAR19-63_z2	zircon	123.4546	32.1377	1.0357	65.0884	39.8401	0.1333	74.4508	0.6324	40.6004	7.1852	0.8105	68.2861
CAR19-63_z3	zircon	125.4800	4.9690	2.1780	144.9479	55.8809	0.2032	158.0799	0.3983	95.2225	24.2811	0.8807	106.2383
CAR19-63_z4	zircon	175.9403	5.6787	1.5882	534.7861	60.4791	0.5327	548.9987	0.1168	411.5353	6.3745	0.7781	55.1181
CAR19-63_z5	zircon	105.0599	2.6387	1.1643	372.8938	197.6002	3.0968	419.3298	0.5475	165.7593	1.8374	0.6914	39.0679
CAR19-66_z1	zircon	101.8189	3.9205	1.2964	211.8903	34.9907	0.6925	220.1132	0.1706	98.5079	9.5454	0.8082	64.4005
CAR19-66_z2	zircon	118.9471	5.9535	1.6693	115.1342	184.1259	1.0811	158.4037	1.6523	86.4236	12.6139	0.8415	83.3290
CAR19-66_z3	zircon	300.7198	26.6695	3.7096	125.4931	140.1285	1.5333	158.4233	1.1537	190.9245	2.9231	0.7248	44.8215
CAR19-66_z4	zircon	71.5560	1.9735	0.6672	272.3742	34.4460	0.5183	280.4690	0.1307	85.3193	6.0038	0.7839	56.7080
CAR19-66_z5	zircon	94.5718	16.5509	1.2561	24.6033	23.1122	0.3031	30.0347	0.9706	12.4679	7.4494	0.8071	67.6022
CAR19-72_z1	zircon	99.6084	6.3806	0.8453	405.5592	119.9780	0.5541	433.7540	0.3057	185.5380	4.4553	0.7897	58.6497
CAR19-72_z2	zircon	134.9585	12.0625	3.9770	0.4980	3.3625	2.1418	1.2882	6.9760	0.7507	6.5902	0.7803	60.0615
CAR19-72_z3	zircon	210.2957	13.5552	2.3957	495.8861	266.6524	3.4043	558.5494	0.5556	516.7891	7.4460	0.8012	62.6400
CAR19-68_z1	zircon	265.0770	6.0549	2.4480	227.7122	135.7231	0.6312	259.6071	0.6158	307.2216	8.1180	0.8092	65.5176
CAR19-68_z2	zircon	152.2001	15.5668	1.5932	737.7957	141.2934	1.2249	770.9996	0.1979	522.2199	8.4707	0.8145	66.7699
CAR19-68_z3	zircon	231.6371	11.3381	1.8068	132.6312	26.8340	0.2381	138.9372	0.2090	146.8286	12.5871	0.8290	72.7415
CAR19-69_z1	zircon	209.2321	34.0198	2.2033	106.0072	12.6138	0.0877	108.9714	0.1229	99.2956	6.1915	0.7929	59.3174
CAR19-69_z2	zircon	97.6811	9.1464	1.4804	124.4586	67.3612	0.3279	140.2885	0.5592	58.5293	6.7173	0.7854	57.7745
CAR19-69_z3	zircon	63.3571	2.7175	0.6286	124.3378	93.4843	0.8481	146.3066	0.7768	39.9275	6.9708	0.7942	60.6918
CAR19-69_z4	zircon	107.1800	4.8733	1.4282	126.1544	87.3496	0.3179	146.6816	0.7154	68.4215	7.0839	0.7996	62.3308
CAR19-69_z5	zircon	43.3743	3.5820	1.8252	0.6895	8.5991	2.9336	2.7102	12.8864	0.5136	9.5696	0.7960	66.0010

S4: Table of raw result for ZHe